Title: Indirect geophysical characterization of geohazards in mantled karst environments (Zaragoza area, Ebro Basin, Spain).

Authors: Pueyo Anchuela, Óscar; Casas Sainz, Antonio Maria; Pocoví Juan, Andrés.

Grupo de Investigación Geotransfer. Universidad de Zaragoza.
opueyo@unizar.es; acasas@unizar.es; apocovi@unizar.es; http://goo.gl/pVuwjj

Abstract

Karst hazards in the central Ebro Basin are related to subsidence and collapses due to solution of evaporitic rocks located several to tens of meters below the surface. In this type of karst (mantle karst) cavities propagate upwards through a non soluble rock, in this case, Quaternary alluvial deposits. The typical geological series comprises a heterogeneous alluvial unit underlain by a soluble, mainly gypsiferous, substratum and several water tables that usually present high conductivity variations. The highest concentration of karstic evidences is identified along the fluvial flood plain of the Ebro River where clayey deposits dominate at surface. These boundary conditions produce complex environments for the evaluation of geophysical data related to i) karst activity, ii) the presence of cavities below the water table and within the substratum and iii) the variable sedimentary architecture of fluvial deposits. During the past 10 years different geophysical techniques have been used in order to characterize karst hazards in the Central Ebro Basin. These experiences have permitted to evaluate resolution, discrimination characteristics and karstic evidences using different approaches. The main success in the application of these geophysical techniques has been the quantification of karst hazards from the record of subsidence processes through changes in density, magnetic susceptibility, apparent conductivity and structure of the alluvial deposits. However, the identification of cavities below the alluvial series represents still a serious handicap due to non-univocal interpretations and low resolution or penetration of geophysical techniques.

Keywords: karst hazards, near surface geophysics, GPR, magnetometry, EM, microgravimetry.

Introduction

Karst terrains are widely exposed worldwide and represent a serious environmental constraint to urban development. Geophysical methods have been commonly used in order to decipher the underground structure during preliminary building planning and the potential future evolution of karst processes below infrastructures. The evaluation of geological factors during planning can define unsuitable sectors or areas where detailed campaigns of geotechnical surveying are required. This approach can permit the engineering adaptation in construction style, foundation types, mitigation measurements or even adaptation procedures to active processes or potential future hazards (e.g. Pueyo Anchuela et al., 2011a; 2013a; 2015a). When the hazardous areas or sectors with high susceptibility to active karstic processes cannot be avoided, dense geotechnical campaigns are required in order to evaluate its presence, extension, and characteristics and to predict future instabilities (Pueyo Anchuela et al., 2014a; 2015b) Geophysical techniques are of particular interest in the joint evaluation of such sectors, integrating methods concerning different properties, resolutions and research depth (Pueyo Anchuela et al., 2010; 2011a and references therein). Moreover, when problems appear after the infrastructure has been built or is in use, the direct characterization can be limited, and indirect approaches can help to the overall definition of the origin of the problem.

The objectives of geophysical surveys in karst terrains have involved i) the evaluation of the potential presence of cavities at different depths in the underground, ii) the detection of decreasing competence of the alluvial cover due to downward migration of material towards cavities or iii) the lack of competence of the very soluble materials. All these approaches have been used to evaluate the origin of the karst phenomenon, and its horizontal and vertical extension, to predict problems in sectors without clear surficial evidences, and also to understand the in-depth origin of identified subsuperficial changes.

In this article we present the experience accumulated by our research group in the evaluation of karst hazard in the central Ebro Basin (NE Spain). In this area surficial evidences or infrastructure affections can be ascribed to different origins, and geophysical methods can help in their understanding. We also evaluate the limits found in the application of geophysical techniques and the routines adopted in order to detect karstic phenomena.

Geological Context

At present, the Ebro Basin is the hydrological basin of the river Ebro and its tributaries, from the geological point of view, the Cenozoic Ebro basin evolved as the foreland to the Pyrenees to the North, the Iberian Chain to the South, and the Catalan Coastal Range to the East (see Fig. 1a). These bounding chains defined a triangle-shaped, endorheic basin that persisted until the Late Miocene reaching an average height of 900-1000 m above sea level. The sedimentary environments defined concentric facies rings related to alluvial systems, with conglomerates in the marginal areas, near the uplifting borders, fluvial systems in the intermediate areas and an evaporite domain in the basin center. Eventually, the Ebro basin was captured during the Late Miocene, developing its recent fluvial network towards the Mediterranean Sea. This process triggered the erosion of the Cenozoic basin that reaches at present an average of 220 m.a.s.l. height in the surroundings of Zaragoza city (located in the central area of the evaporitic basin). In the Zaragoza area, karstic processes have been contemporary with Quaternary erosion and sedimentation. As a result, the position of the evaporite-alluvial contact can be 100 m below the thalweg (e.g. Benito et al., 2000, Pueyo Anchuela et al., 2013b).

A widespread mantled karst has progressed associated with the Quaternary fluvial terraces of the Ebro River and its tributaries (fig. 1b). This type of karst develops in the presence of mainly gypsum (Fig. 1c), but also other more soluble salts, such as glauberite and halite, that have been identified at boreholes and mining activities (Salvany, 2009). Salt levels can be located from some meters to several tens of meters below non soluble, detrital materials (Pueyo Anchuela et al., 2013b). Therefore, the origin of the problem is located below a thick cover of alluvial, non soluble deposits (Fig 1d) and the surficial karst evidences, including collapses and subsidence (Fig. 2), depend also on the rheology of the cover (e.g. Pueyo Anchuela, 2015a). Moreover, secondary karst, piping, settlement or soil collapses are associated with Quaternary deposits linked to pediments having high contents of evaporitic detrital materials (e.g. gypsum silts; see Pueyo Anchuela et al., 2014b). The continuous interaction of sedimentation and active karstic processes during the Quaternary has also favored the development of anomalous geometries in certain deposits, or unusual facies within Quaternary terraces (e.g. Luzón et al., 2008; Pueyo Anchuela et al., 2014c).

Geological-Geophysical model. Problem definition.

Geological features vary laterally along the studied area, but some general considerations can be established. A vertical stratigraphical/geotechnical profile from bottom to top consists of: i) Neogene, mainly Miocene evaporitic materials (Fig. 1c), ii) weathered substratum and soils, usually grey marls iii) alluvial-colluvial deposits (Fig 1d) and iv) recent soils. In general, recent and agricultural soils are scarce and only show significant development on the alluvial flood plain (Fig. 1c and d). The geotechnical profile can be complicated by several water tables: a confined saline aquifer in the substratum, and unconfined aquifers related to both irrigation and the Ebro River.

The characterization of the alluvial deposits as indicative of active processes has been used in order to infer karst activity developing below the depth commonly reached by geophysical techniques. This approach requires dense surveys in order to reconstruct sedimentary architecture and evaluate anomalies due to karst processes (e.g. Pueyo Anchuela et al., 2009). From a geophysical point of view, the determination of properties of the involved units can permit, in a preliminary approach, the evaluation of the potential applicability of geophysical techniques to mantle karst (e.g. Pueyo Anchuela et al., 2010; 2011b). This includes, for example, diamagnetic behavior of cavities, strength or density decrease of underground materials and alluvial decompaction, resistivity anomalies or hyperbolic anomalies in radargrams over cavities or collapsed structures. However, a strict definition of the context is necessary to define the limits of each technique due to complex alluvial structures, syn-sedimentary karst activity, depth of cavities and changes related to the water tables and their geochemical characteristics.

In the following sections we include some examples where the depth to the target (cavities) could not be reached, but the sedimentary alluvial architecture permitted to infer the presence of karstic features. Surveys were carried out by the Geotransfer research Group from the University of Zaragoza, whose target in this field has been the integration of magnetometry, microgravimetry, seismic refraction, electromagnetic multifrequency surveys, ERT and GPR.

Inferring karst phenomena from the anomalous sedimentary filling of collapses or subsidence areas.

In many cases active karstic domains, including collapses and subsidence areas can be topographically leveled either by river flooding or human farming activities. The identification of previous karstic processes from historical aerial photographs, farmers' interviews and geomorphological sources can be of high interest in the evaluation of previous processes that can be partially masked at the moment of geophysical surveying.

Natural and anthropogenic filling of subsidence and collapse features produce different signatures accordingly to the involved materials. Natural fillings consist usually of clay deposits whereas anthropogenic materials include remobilized soils or non natural materials including urban debris. Over these fillings, gravimetry can show irregular behavior and changes of the Bouguer anomaly at the vertical of the depth changes of the consolidated unit. Magnetic anomalies clearly reveal collapses when they are filled by waste materials (Mochales et al., 2008). Apparent conductivity anomalies revealed by EM variable frequency surveys are scarce and more dependent on the filling that on the underlying cavities. Commonly, the apparent conductivity anomalies decrease in size with depth (Fig.3b to d), in agreement with the conical geometry of the upward propagation of the perturbation. In the analyzed collapse (figs. 3, 4), the amplitude and wavelength of the anomaly is related to the anthropogenic filling (Fig. 3e and 4 b). Microgravimetric data locate the vertical pipe more accurately, but the conical shallow geometry can be better defined by GPR, permitting the identification of the sinkhole limits. However, soil characteristics in flood plain environments significantly reduce wave penetration, thus limiting the identification of the in-depth origin of dolines (fig. 4c).

Something similar can be found in the case of subsidence areas (Fig. 5), although the thickness of the filling can be lower. In these settings, the higher proportion of clay deposits, presence of water and the subdued topography favor vegetation growth (Fig. 5a). These factors contribute to an increase in conductivity (Fig. 5c to f), defining an anomaly whose wavelength decreases with depth. Magnetic dipoles surround the subsidence area (fig. 6c and d) and their identification is not as direct as in the collapses because of their smaller amplitude. The filling and higher clay content in the inner domain of the subsidence area also can be detected by means of GPR but to shallower depths than necessary for identifying the actual origin of the problem (Fig. 6e).

Inferring karst phenomena from the anomalous architecture of underground materials in urban domains.

The indirect characterization of karst phenomena through the structure and behavior of the alluvial deposits provides indirect insights to evaluate karst phenomena. However, detection of changes in material properties can be significantly limited at urban domains due to geophysical noise. This restricts the application of magnetic and electromagnetic techniques in certain contexts. GPR is useful for evaluating deformation and reparations of constructive levels that can be also interpreted according to their geometrical features (e.g. Pueyo Anchuela et al., 2014a).

In fig. 7 we show several examples of radargram interpretation, taking into account the definition of GPR domains. Similar low penetrations are reached with different GPR antennas due to natural penetration barriers. Detailed analysis is focused on the distribution of homogeneous constructive structures with respect to the non horizontal or heterogeneous domains. In the profile shown in fig. 7a, three different domains submitted to subsidence and continuous reparations can be identified. Subsequent excavation permitted to observe three levels of constructive pavements, as well as thickness changes in the asphalt layers. On the other hand, in urban domains, similar penetrations can be achieved with high-frequency antennas, permitting detailed analysis to be carried out at the most shallow constructive levels. In the case of fig. 7c, a collapse geometry and reparations affected by recent subsidence processes can be identified, with similar penetration for 250 MHz and 100 MHz (fig. 7d).

Synthesis and conclusions.

Shallow subsurface geophysical surveys in different sectors of the Central Ebro Basin show the difficulties in the evaluation and interpretation of the origin of karstic processes, often unapproachable by usual techniques. However, the possibility to infer its presence by means of the analysis of the structure in the overlying levels (geometry and geophysical behavior) supports the possibility of their evaluation through their effects at the alluvial series. This approach does not permit the identification of cavities in a univocal manner, what would require deep boreholes and geophysics in cross-hole and down-hole essays. However, the possibility to define the 3D geometry of affected materials from the few upper meters support the applicability of shallow subsurface geophysics in order to improve underground knowledge of karst activity.

While in some cases penetration depth can limit the identification of the underground origin, in certain sectors the geometry and shape of the anomalies, and the appearance of the non-affected units at depth, can permit to infer the karst origin, especially when several mechanisms can be expected (e.g. settlement, soil collapse, piping or deep karstic solution processes, e.g. Pueyo Anchuela et al., 2014b).

These data support the applicability of the indirect characterization of karst phenomena through changes related to the record of the karst activity both by natural and anthropogenic deposits. This approach is of application even without reaching the origin of the problem, but the success in the prediction of new subsidence foci is limited if they are in the substratum, below conductive levels or associated with reverse strength geotechnical profiles.

Acknowledgements.

This research has been supported by Geotransfer Research Group from University of Zaragoza and applied research agreements with different companies including mainly Geoscan SLP, Control 7 and Zeta Amaltea.

References

Ayala Carcedo, F.J., Rodríguez Ortiz, J.M., del Val Melus, j., Durán Balsero, J.J., Prieto Alcolea, C., Rubio Amo, J. [1986] Mapa del karst en España. Escala 1:000.000. Instituto Geológico y Minero de España. Madrid.

Benito, G., Gutiérrez, F., Pérez-González, A., Machado, M.J. [2000]. Geomorphological and sedimentological features in Quaternary fluvial systems affected by solution induced subsidence (Ebro Basin, NE-Spain). Geomorphology 33, 209–224.

Luzón, M.A., Pérez, A., Soriano, M.A., Pocoví, A. [2008]. Sedimentary record of Pleistocene paleodolines evolution in the Ebro Basin (NE Spain). Sedimentary Geology 205, 1–13.

Mochales, T., Casas, A.M., Pueyo, E.L., Pueyo, Ó., Román, M.T., Pocoví, A., Soriano, M.A., Ansón, D. [2008]. Detection of underground cavities by combining gravity, magnetic, and ground penetrating radar: a case study from the Zaragoza area, NE Spain. Environmental Geology, 53, 1067-1077.

Pueyo Anchuela, Ó., Casas Sainz, A.M., Soriano, M.A., Pocoví Juan, A. [2009]. Mapping subsurface karst features with GPR: results and limitations. Environmental Geology, 58, 391-399.

Pueyo Anchuela, Ó., Casas Sainz, A.M., Soriano, M.A., Pocoví Juan, A. [2010] A geophysical survey routine for the detection of doline areas in the surroundings of Zaragoza (NE Spain). Engineering Geology 114, 382-396.

Pueyo Anchuela, Ó., Casas Sainz, A.M., Soriano, M.A., Pocoví Juan, A. [2011a]. Geophysical techniques applied to urban planning in complex near surface environments. Examples of Zaragoza, NE, Spain". Physics and Chemistry of the Earth, 36, 1211-1227.

Pueyo Anchuela, Ó., Casas Sainz, A.M., Pocoví Juan, A., Ansón López, D. [2011b]. Multidisciplinary approach for urban planning over alluvial karstic zones. Case study from the Central Ebro Basin (Spain)". Engineering Geology, 122, 222-238.

Pueyo Anchuela, Ó., Pocoví Juan, A., Casas Sainz, A.M., Ansón López, D., Gil, H. [2013a]. Actual extension of sinkholes: Considerations about geophysical, geomorphological, and field inspection techniques in urban planning projects in the Ebro basin (NE Spain). Geomorphology, 189, 135-149.

Pueyo Anchuela, Ó., Gil, H., Ramajo, J., Ipas, J.F., Simón, J.L., Ansón, D., Gracia, J. [2013b]. Distribución de los espesores del aluvial de la zona de Zaragoza, análisis de la influencia kárstica. Geogaceta, 53, 113-116.

Pueyo Anchuela, Ó., Casas Sainz, A.M., Pocoví Juan, A., Gil Garbí, H., Calvín, P. [2014a]. Characterization of the karstic process in an urban environment using GPR-surveys. Journal of Materials in Civil Engineering 26 (8), 05014004.

Pueyo Anchuela, Ó., Pocoví Juan, A., Bartolomé, J.I., Casas-Sainz, A.M., Revuelto, C., Galindo, G. [2014b]. Propuesta de integración de análisis de patologías constructivas con prospección geofísica por georradar. Geogaceta, 55. 71-74.

Pueyo Anchuela, Ó., Luzón, A., Gil Garbí, H., Pérez, A., Pocoví, A., Soriano, M.A. [2014c]. Combination of electromagnetic, geophysical methods and sedimentological studies for the development of 3D models in alluvial sediments affected by karst (Ebro Basin, NE Spain). Journal of Applied Geophysics, 102, 81-95.

Pueyo Anchuela, Ó., López Julián, P., Liesa, C.L., Casas Sainz, A.M., Pérez Benedicto, J.A., Pocoví Juan, A., Ramajo Cordero, J. [2015a]. Three dimensional characterization of complex mantled karst structures. Decision making and engineering solutions applied to a road overlying evaporite rocks in the Ebro Basin (Spain). Engineering Geology, 193: 158-172.

Pueyo Anchuela, Ó., Casas Sainz, A.M., Pocoví Juan, A., Gil Garbí, H. [2015b]. Assessing karst hazards in urbanized areas. Case study and methodological considerations in the mantle karst from Zaragoza city (NE Spain). Engineering Geology, 184, 29-42.

Salvany, J.M. [2009]. Geología del yacimiento glauberítico de Montes de Torrero (Zaragoza). Ed. Universidad de Zaragoza. 80 p.

Figure Captions.

Figure 1.- a) Map of the Iberian peninsula showing materials susceptible of karstification (carbonatic and evaporitic rocks; modified from Ayala et al., 1986). b) Field photograph where evaporites and terrace-flood plain levels can be identified, c) outcrop of evaporitic gypsum unit, d) aerial view showing the main geological units (from google earth image).

Figure 2.- Some common evidences of karst activity related to cavity propagation up to the surface both in natural and anthropogenic environments, including collapses (a,b) and subsidence phenomena affecting to urban structures (c,d,e,f).

Figure 3.- Perspective view of a karst collapse including: a) aerial photograph, b,c,d); apparent conductivity anomalies for different depths and e) magnetic dipole generated by the collapse filling.

Figure 4.- Comparative analysis of a) aerial photograph, b) magnetic vertical gradient identified over a collapse filled with urban debris and c) sketch showing the magnetic anomaly, microgravimetric anomaly and GPR profiles along two normal directions.

Figure 5.- Presentation in perspective view of a subsidence sinkhole including a) aerial photograph, b) topographic map and c,d,e,f) apparent conductivity maps for different depths.

Figure 6.- Comparative analysis of a) aerial photograph, b) topography, c,d) intensity and vertical magnetic gradient of the Earth's Magnetic field and e) GPR profile along the central part of the subsidence sinkhole (see b for location).

Figure 7.- GPR profiles in urban domains where structural anomalies involving constructive materials are marked. In a), the inhomogeneous marked sector corresponds to the excavated area in the photograph shown in b). c, d) show the profiles carried out with 250 and 100 MHz antennas where the same collapse geometry at a subsidence surficial area is marked (250 MHz profile corresponds to the marked sector at d).

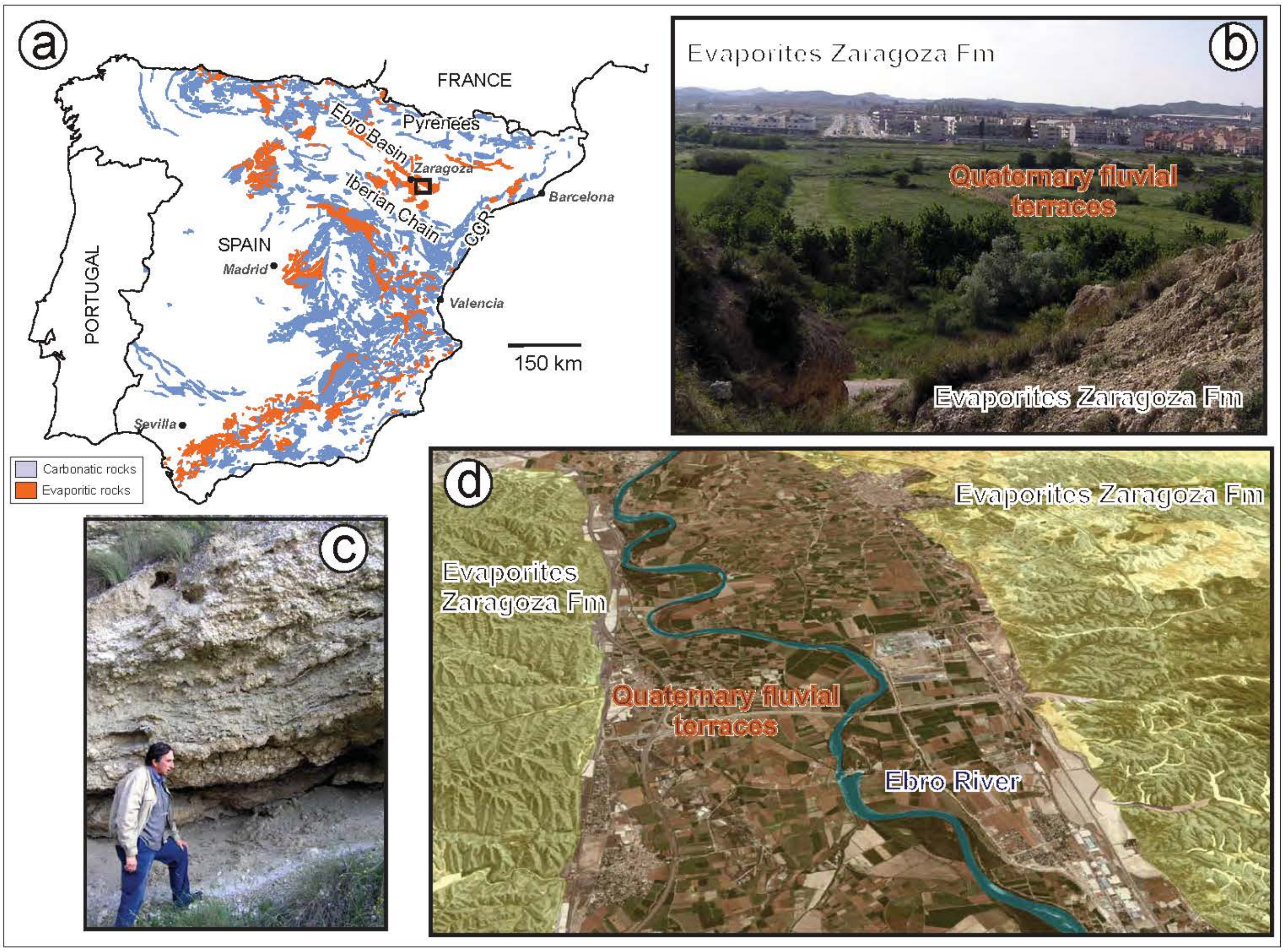
a
FRANCE
Pyrenees
Ebro Basin
Zaragoza
Iberian Chain
CCR
Barcelona
SPAIN
Madrid
PORTUGAL
Valencia
150 km
Sevilla
Carbonatic rocks
Evaporitic rocks
b
Evaporites Zaragoza Fm
Quaternary fluvial terraces
Evaporites Zaragoza Fm
c
d
Evaporites Zaragoza Fm
Evaporites Zaragoza Fm
Quaternary fluvial terraces
Ebro River

Figure 1.-

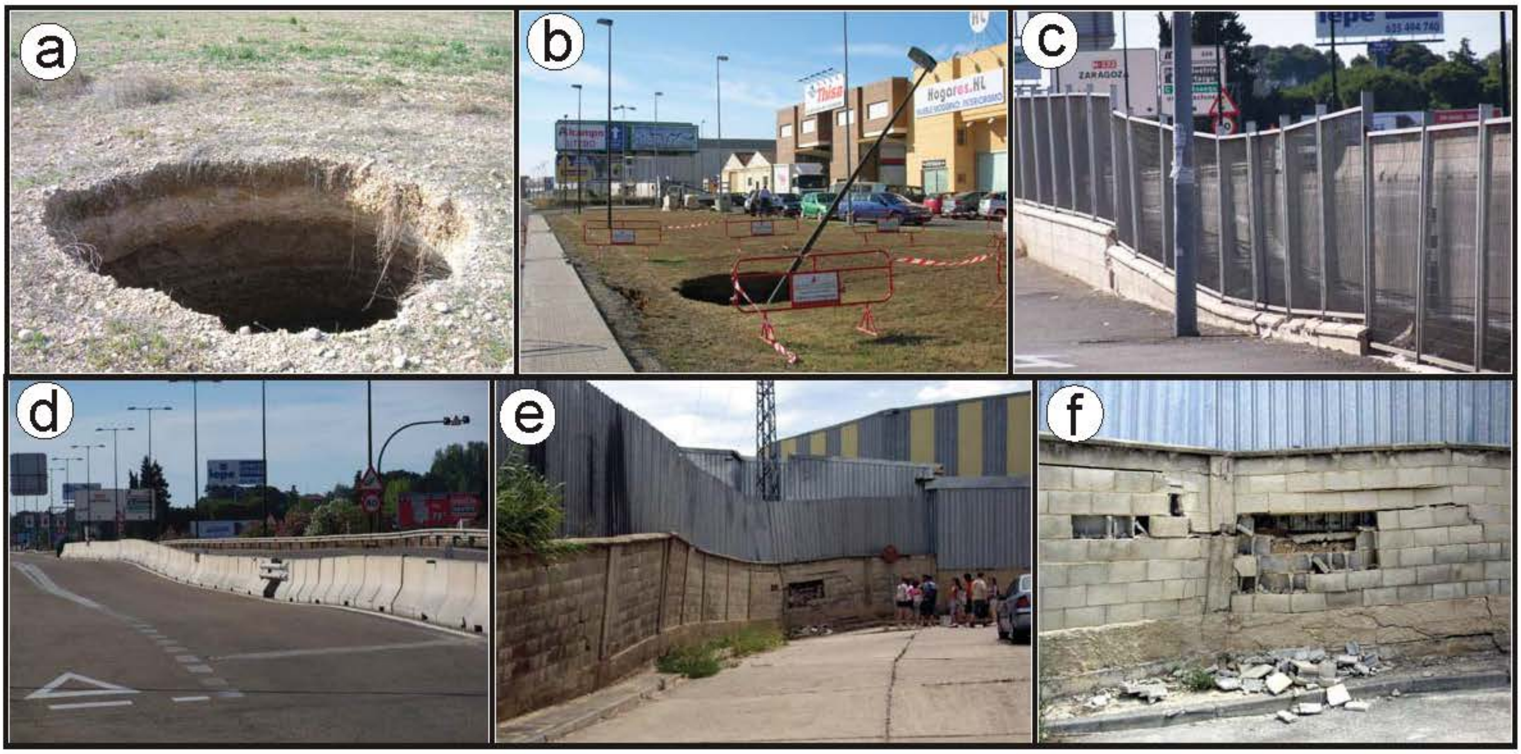

Figure 2.-

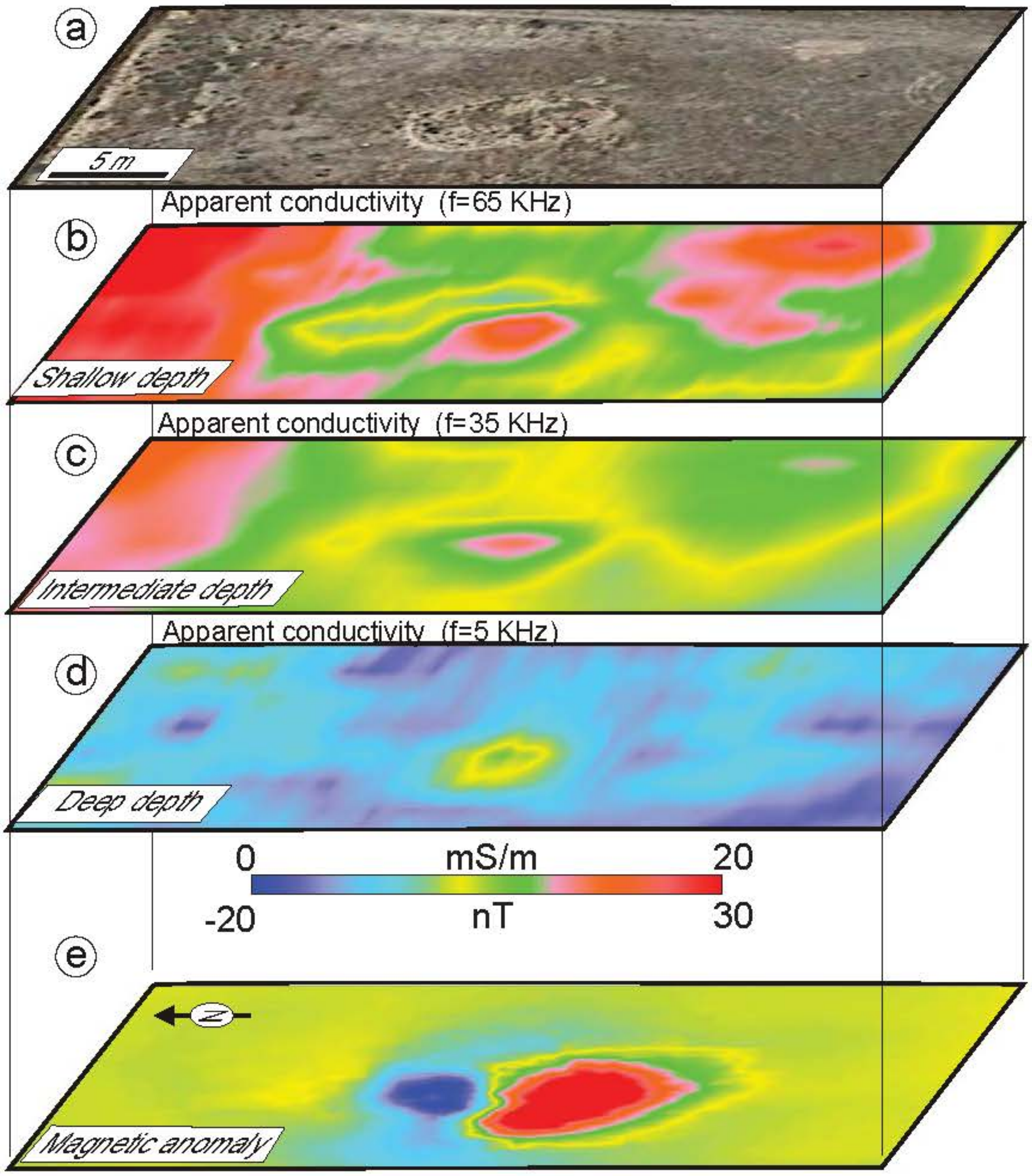
a
5 m
Apparent conductivity (f=65 KHz)
b
Shallow depth
Apparent conductivity (f=35 KHz)
c
Intermediate depth
Apparent conductivity (f=5 KHz)
d
Deep depth
0
mS/m
20
-20
nT
30
e
N
Magnetic anomaly

Figure 3.-

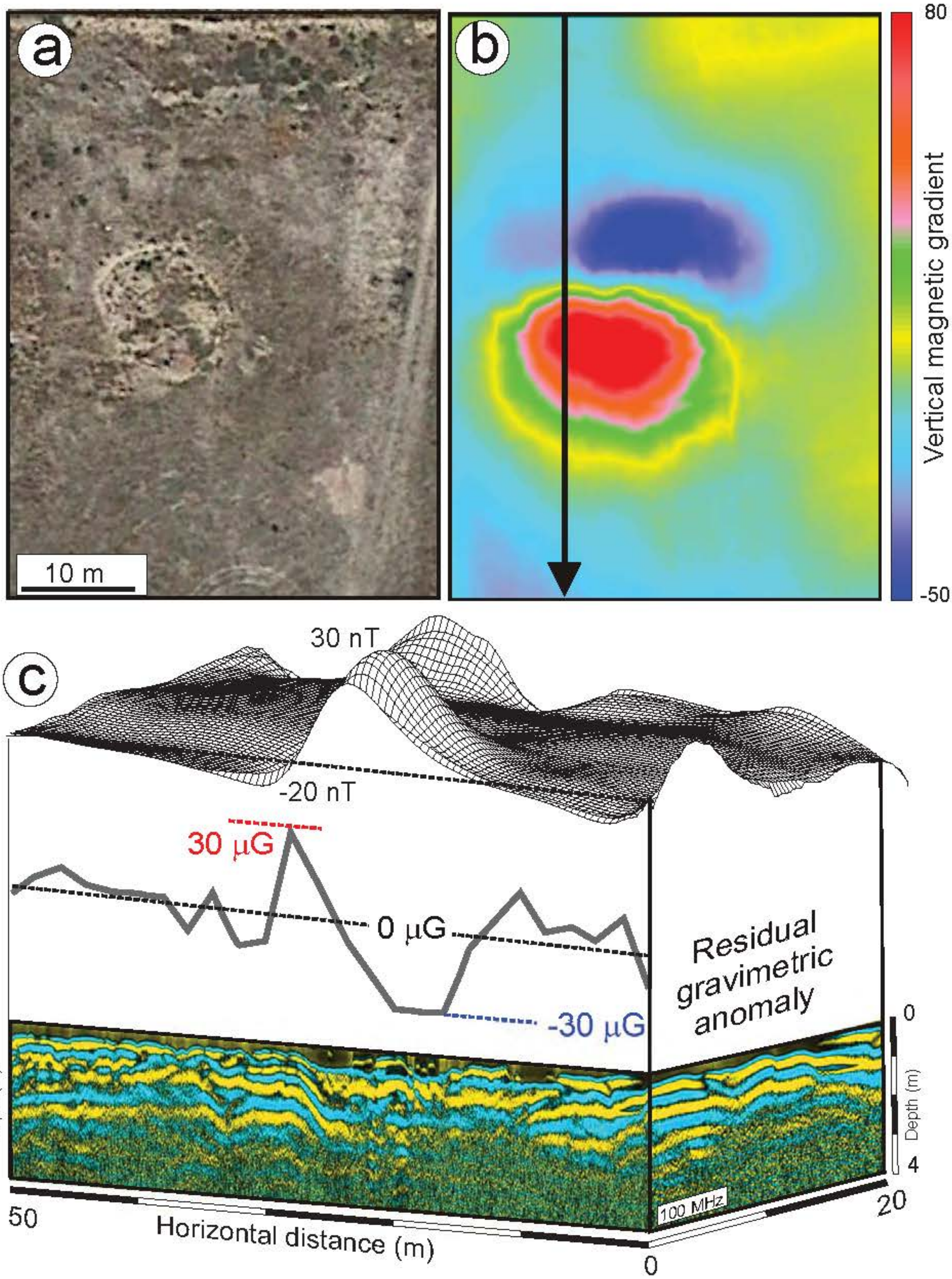

a
10 m
b
80
Vertical magnetic gradient
-50
c
30 nT
-20 nT
30 μG
0 μG
-30 μG
Residual
gravimetric
anomaly
Depth (m)
0
4
100 MHz
50
Horizontal distance (m)
0
20

Figure 4.-

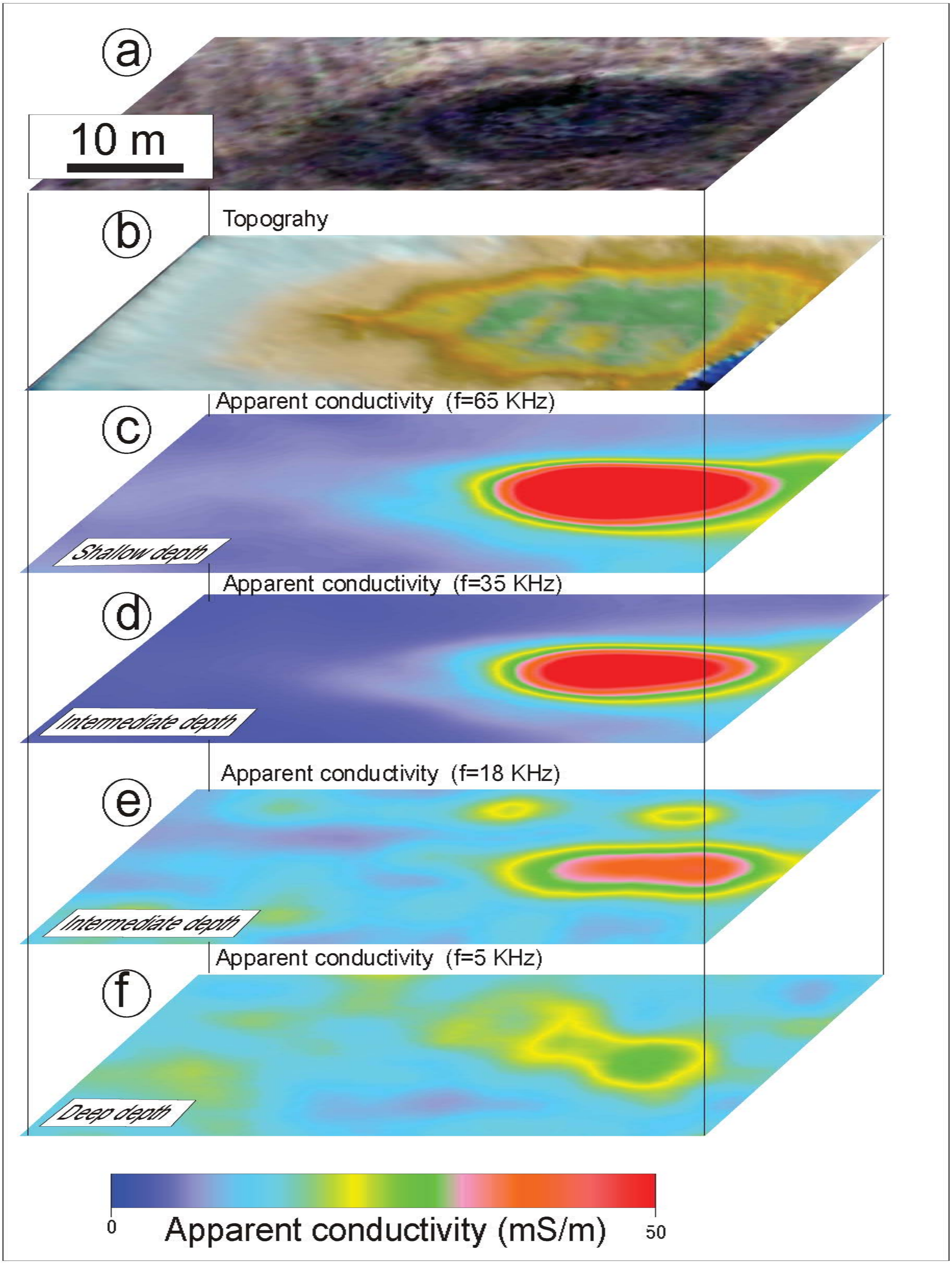
a
10 m
b
Topograhy
Apparent conductivity (f=65 KHz)
c
Shallow depth
Apparent conductivity (f=35 KHz)
d
Intermediate depth
Apparent conductivity (f=18 KHz)
e
Intermediate depth
Apparent conductivity (f=5 KHz)
f
Deep depth
0
Apparent conductivity (mS/m)
50

Figure 5.-

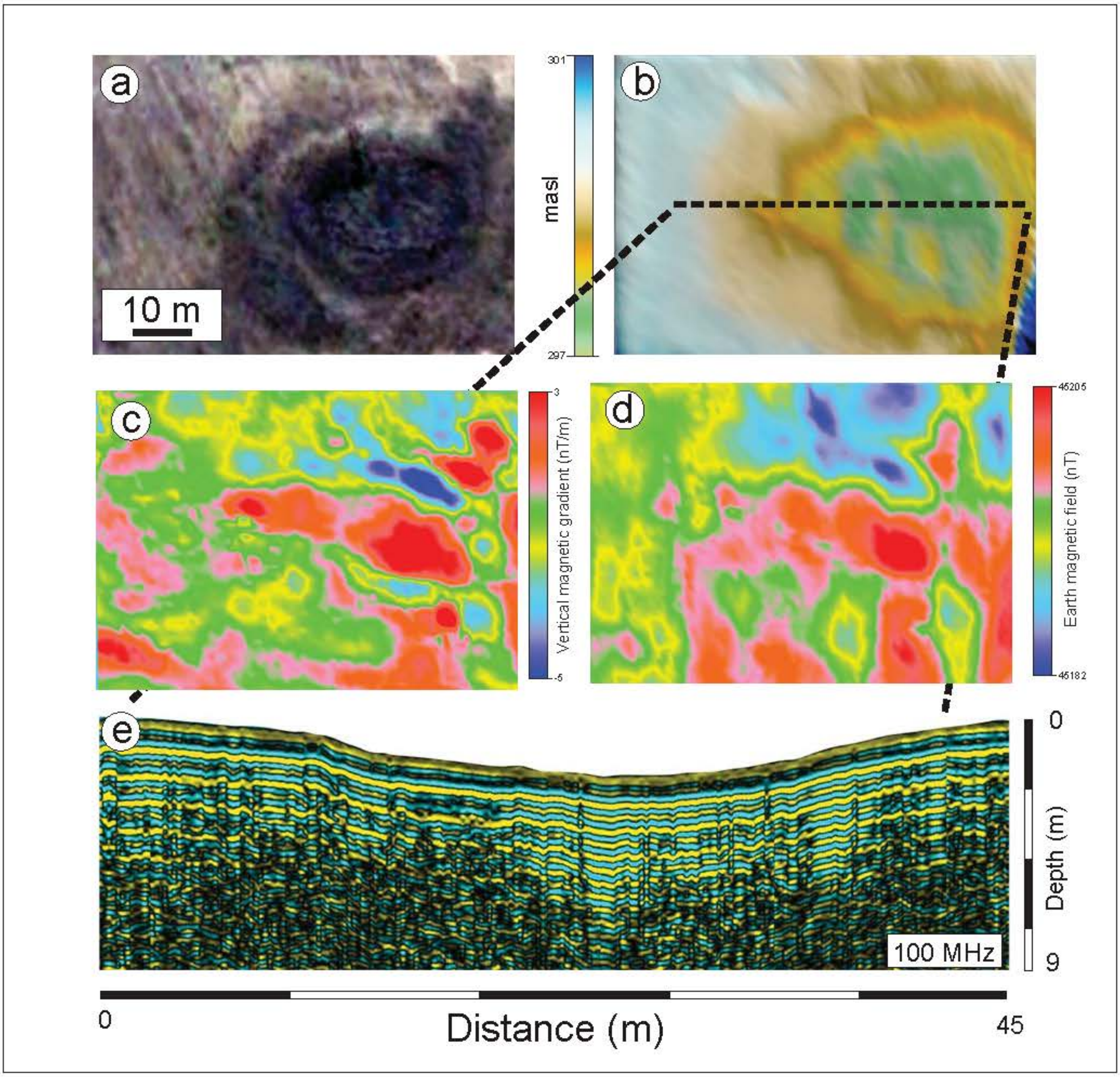
a
10 m
b
301
masl
297
c
3
Vertical magnetic gradient (nT/m)
-5
d
45205
Earth magnetic field (nT)
45182
e
0
Depth (m)
9
100 MHz
0
Distance (m)
45

Figure 6.-

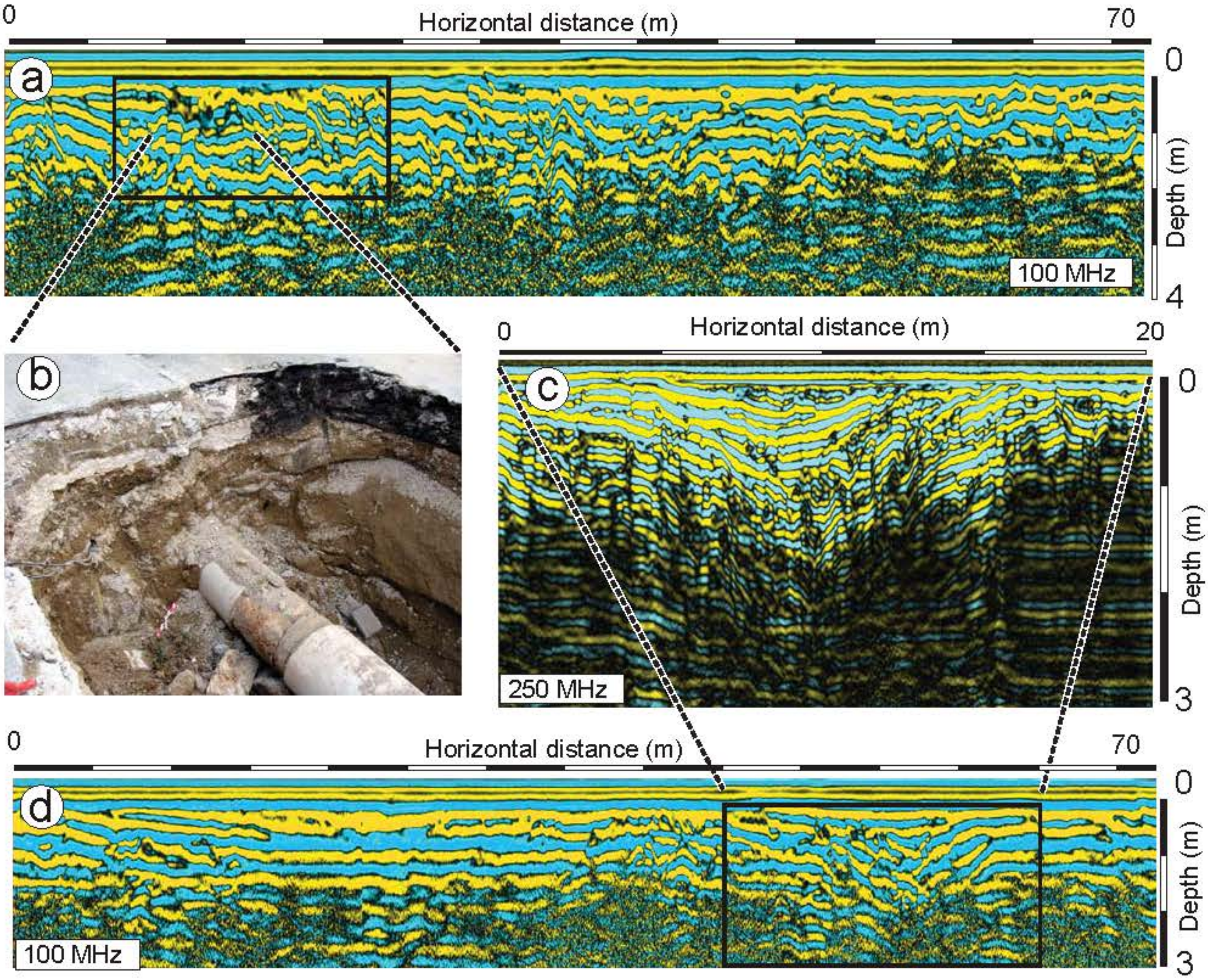

0
Horizontal distance (m)
70
a
0
Depth (m)
4
100 MHz
b
0
Horizontal distance (m)
20
c
0
Depth (m)
3
250 MHz
0
Horizontal distance (m)
70
d
0
Depth (m)
3
100 MHz

Figure 7.-